

Factors That Affect Radiofrequency Heat Lesion Size

Eric R. Cosman Jr, PhD,* Joseph R. Dolensky, BS,[†] and Ryan A. Hoffman, BS[†]

*Cosman Medical, Burlington, Massachusetts;

[†]Department of Biomedical Engineering, Georgia Institute of Technology, Atlanta, Georgia, USA

Reprint requests to: Eric R. Cosman Jr, PhD, Cosman Medical, 76 Cambridge Street, Burlington, MA 01803, USA. Tel: +1-781-272-6561; Fax: +1-781-272-6563; E-mail: ercosman@alum.mit.edu.

Disclosure: Funding provided by Cosman Medical. Eric Cosman is a shareholder of Cosman Medical.

Abstract

Objective. This study aims to compare radiofrequency (RF) heat lesion size across electrodes and generator settings available for interventional pain management.

Methods. Monopolar lesions are generated *ex vivo* in animal tissue using sharp cannulae with tip diameters 23, 22, 20, 18, 16 gauge; tip lengths 5, 6, 10, 15 mm; set temperatures 60, 70, 80, 90°C; set times 1, 1.5, 2, 3, 5, 10 minutes. Lesions are generated using the RRE electrode, cooled RF, and parallel-tip bipolar RF for comparison. Lesion sizes are assessed by automated photographic temperature inference from over 400 lesions, using multiple lesions per configuration.

Results. Monopolar lesion width and length increase with each factor ($P < 0.001$). Increasing cannula diameter from 22 to 16 gauge increases average lesion width 58–65% (3–4 mm) at 80°C and 2 minutes. Increasing temperature from 60°C to 90°C increases lesion width 108–152% at 2 minutes. Although dimensions grow most rapidly over the first minute, average lesion width is 11–20% larger at 2 minutes, and 23–32% larger at 3 minutes, compared with 1 minute. Lesion length extends distal and proximal to the tip, and exceeds tip length by 1–5 mm at 80°C and 2 minutes. Conventional 16

gauge cannulae at 80–90°C for 2–3 minutes generate lesions of average width similar to that produced by the cooled RF configuration proposed for sacroiliac joint denervation. Bipolar RF between parallel cannulae produces a rounded brick-shaped lesion of comparable shape to three sequential monopolar lesions generated using the same cannulae and generator settings.

Conclusions. Tip gauge, tip length, temperature, and time substantially affect RF lesion size.

Key Words. Radiofrequency; Ablation; Neurotomy; Spine; Sacroiliac Joint; Cooled RF; Bipolar RF

Introduction

The application of radiofrequency (RF) signals to neural tissue is well established in the treatment of movement, mood, and chronic pain disorders [1,2]. Undesired neural signals, such as those transmitting nociceptive pain, are interrupted when high-frequency current (100–1,000 kHz) flowing through an RF probe's active tip raises the temperature at a soma/ganglion or axon/nerve to destructive levels (≥ 45 – 50°C) by means of frictional heating [3–9]. The process is known as RF heat lesioning, RF thermocoagulation, RF ablation, or thermal RF. The volume of tissue damaged by RF heating is called a heat lesion. Monopolar RF refers to current flow between a probe electrode and a large area ground pad placed on the skin's surface. Bipolar RF refers to current flow between two probe electrodes without a ground pad. RF heat lesioning includes cooled RF, wherein the electrode is internally cooled by circulating fluid but surrounding tissue is exposed to destructive temperatures [10–13].

An understanding of the factors that affect RF heat lesion size and shape is critical for selection of generator and probe configurations that suit patient anatomy and clinical objectives. Lesion geometry determines the extent and likelihood of desired and undesired tissue damage given the active tip's position and orientation in patient anatomy. Lesion size thus pertains to the degree and likelihood of interventional success, complications, the number of required lesions, methodological difficulty, procedure time, radiation exposure from fluoroscopic

guidance, tissue damage due to probe manipulation, intra- and post-procedure pain.

In their 1953 publication, W. H. Sweet and V. H. Mark showed the advantage of high-frequency alternating current over direct current in producing well-circumscribed lesion borders with control of size and shape [14]. Studies from the 1950s and 1960s established that RF heat lesion geometry depends reproducibly on electrode shape, tip diameter/gauge (ga), tip length, tip temperature, and lesion time (Figure 1A) [15–17]. The earliest RF lesion generators built by B. J. Cosman, S. Aranow, and O. A. M. Wyss in the early 1950s have been developed into modern tools that automatically control lesion temperature and time (Figure 2A). Monopolar RF lesion size using temperature-controlled neurosurgical and pain management electrodes from the 1950s through the 1980s has been evaluated clinically [18], with *in vivo* animal models [4,17,19,20] and *ex vivo* models [20–23]. However, the variety of probe sizes has grown considerably since the 1980s when the invention of the fine-gauge thermocouple (TC) electrode by E. R. Cosman Sr. [24] enabled variously sized RF cannulae to be electrified and monitored by a separate, universal, temperature-sensing RF electrode (Figure 3). Monopolar RF heat lesioning using a wide variety of sharp, bevel-tip cannula is currently the norm in interventional pain management. Bipolar RF and cooled RF modalities are also common. Over the years, this expansive range of RF methods has been studied incrementally using disparate experimental models, confounding evaluation of the effects of probe size, generator settings, and modality on RF lesion geometry.

The aim of the present study is to compare RF heat lesion size across a broad range of active tip diameters, active tip lengths, set temperatures, set times, and modalities presently available for interventional pain management. The study is intended to evaluate typical cannula and generator configurations, configurations that maximize lesion size, the RRE “Ray” electrode, cooled RF, and bipolar RF under controlled conditions.

Methods

The *ex vivo* animal tissue model used for lesion generation is similar to that described in Cosman and Gonzalez [25], but lesion size measurement is automated in order to analyze a wide variety of probe and generator configurations without human measurement error. Fresh adult bovine liver is frozen, sliced into slabs of approximately 2.5-cm thickness, equilibrated to room temperature within plastic sheets to preserve moisture (average 24°C, std. dev. 1.8°C), and selected for freshness and color. To assess the width W and length L of monopolar and bipolar lesions (Figure 1), cannulae/electrodes are inserted through the top surface of a first slab to fix tip position, and a second slab is placed firmly atop the first, so tissue completely surrounds the active tips. To assess the depth D of bipolar lesions (Figure 1B), vertical cannulae penetrate the two slabs perpendicularly such that the slab

interface is aligned with the middle of cannulae tip lengths. Each electrode is connected to one of the four output jacks of an RF generator (Cosman G4 version 2.1.0, Cosman Medical, Inc., Burlington, MA, USA). For monopolar lesions, the lower slab is positioned on a stainless steel sheet connected to the generator’s reference jack. For bipolar lesions, the lower slab is positioned on an electrically insulative plastic sheet. The generator automatically adjusts the amplitude of a 480-kHz sinusoidal signal to control a monopolar active tip, or the hotter of two bipolar active tips, to within 2°C of the target temperature. The generator stores measurements once per second, including electrode tip temperatures, temperature probe signals, impedance, RMS voltage, RMS current, and average power output. After heating, the top slab is removed when the electrode has cooled to 33°C.

A photograph is taken from directly above the lesion in the lower slab with the cannulae/electrodes and a metric ruler atop it (f/16, 0.6 seconds, RAW format, Canon EOS 20D, Canon USA Inc., Lake Success, NY, USA; Canon EF 100 mm f/2.8 Macro Lens). Illumination is provided by diffused 5,000 K fluorescent lamps. The RAW-format lesion photo is reformatted as TIFF using dcrw v.9.06 (David J. Coffin, Milton, New Hampshire, USA) and imported into MATLAB (Release 2012a, The Mathworks, Inc., Natick, MA, USA). To control for color variations across tissue samples, each photograph is color corrected using a supervised algorithm for identification of raw and central-lesion tissue colors. Each pixel is assigned to one of seven clusters by k-means clustering of RGB color values (MATLAB Statistics Toolbox). A raw-tissue cluster and a central-lesion cluster are selected based on the locations of their constituent pixels, and the mean RGB values of these clusters are assigned as the raw \mathbf{r} and central-lesion \mathbf{c} tissue colors, respectively. Each pixel’s RGB color \mathbf{x} is projected onto the line segment passing through the raw \mathbf{r} and the central-lesion \mathbf{c} RGB values. Electrodes and specular highlights are segmented by zeroing projection coefficients greater than 1.5, and each pixel is mapped to a normalized scalar “color index” $p = \text{sat}((\mathbf{x}-\mathbf{r}) \cdot (\mathbf{c}-\mathbf{r}) / |\mathbf{c}-\mathbf{r}|^2, 0, 1)$ that linearly parameterizes the line segment (Figure 2D), where $\text{sat}(x, y, z)$ saturates x at the lower y and upper z bounds.

To calibrate tissue color change to the thermal damage that accrues with elevated temperature over time [26], a preliminary series of 40 large bipolar lesions are generated in multiple tissue samples using 80°C/3 min or 90°C/3 min generator settings and 20 ga/15 mm sharp-tip cannulae/electrodes (Cosman CC101520, TCN-10) spaced by approximately 15 mm. Tissue color is matched to final tissue temperature by measurement at a variety of locations using fine-gauge, electrically passive probes (Figure 2B), each consisting of an electrically-insulated TC electrode (Cosman TCN-10, 0.36 mm diameter) connected to a generator jack with disconnected RF lines. The color index p at the probe’s sensor location is found to correlate to the final probe temperature, to produce contrast between baseline and minimal neurolytic temperatures (45–50°C) and to saturate at approximately

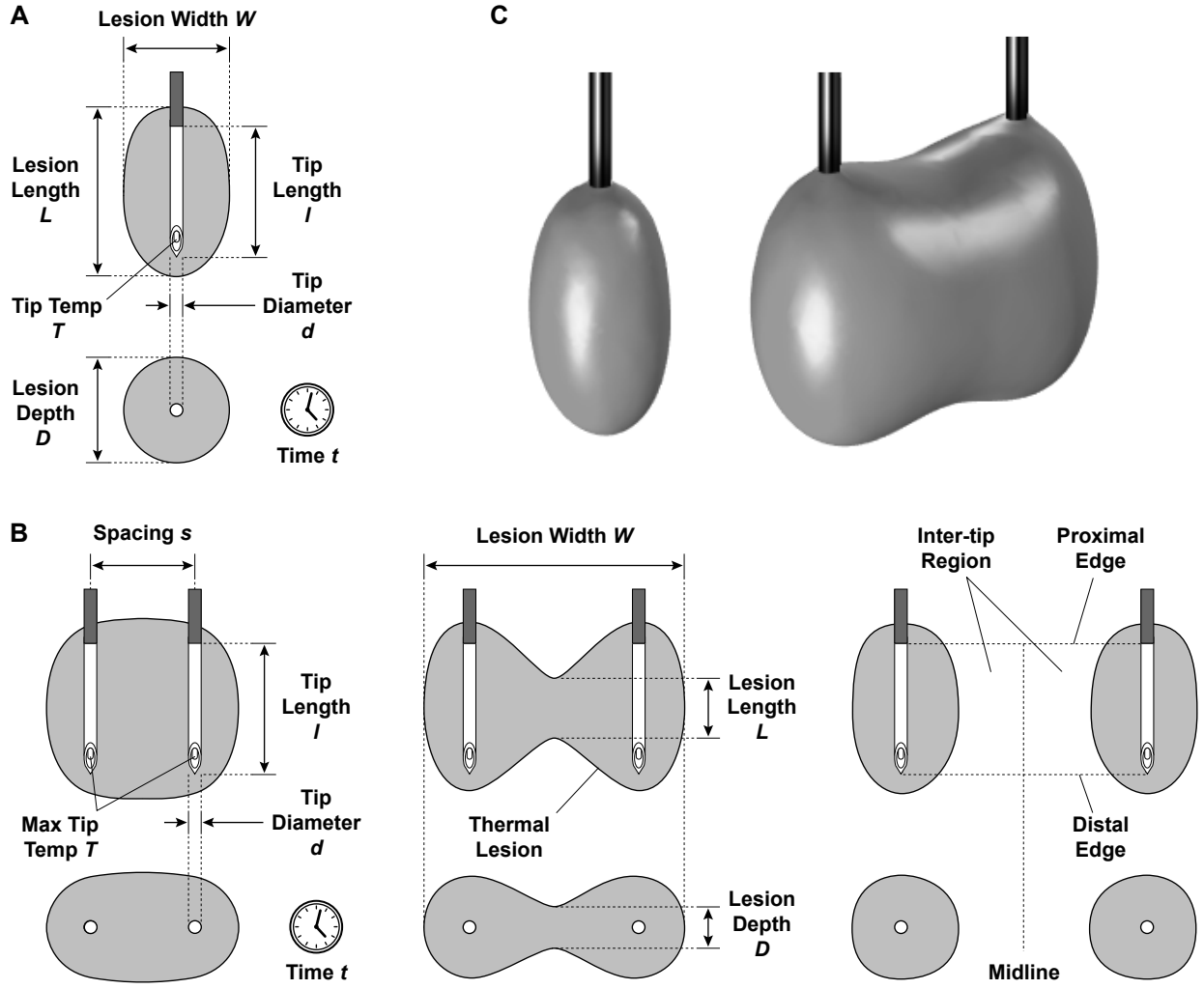


Figure 1 RF heat lesion size measurement and influencing factors. Each panel shows a single lesion in longitudinal (top) and axial (bottom) cross sections. (A) Monopolar lesions are egg-shaped with length L measured in the active tip's longitudinal direction, and lesion width W and depth D in the tip's radial direction. Lesion width W and depth D are approximately equal due to the active tip's predominant radial symmetry. Lesion size depends on tip diameter/gauge d , tip length l , tip temperature T , and lesion time t . (B) Bipolar lesions are additionally influenced by the inter-tip spacing s . The electric field and current density responsible for RF heating are more intense between closer tips. As tip spacing s increases from left to right in the three examples shown, the lesion expands in width W and narrows in both length L and depth D at the midline. For nearby, roughly parallel tips, bipolar lesions have a rounded brick shape. At large distances, bipolar lesions have approximately monopolar shape. The range of spacing values s over which this transition occurs depends on the other configuration parameters l , d , T , and t [25]. (C) Three-dimensional rendering of the 55°C isotherm from electrothermal finite-element models [44] of monopolar RF 18 ga/10 mm/80°C/2 min (left) and bipolar RF 18 ga/10 mm/90°C/3 min with 12 mm spacing (right).

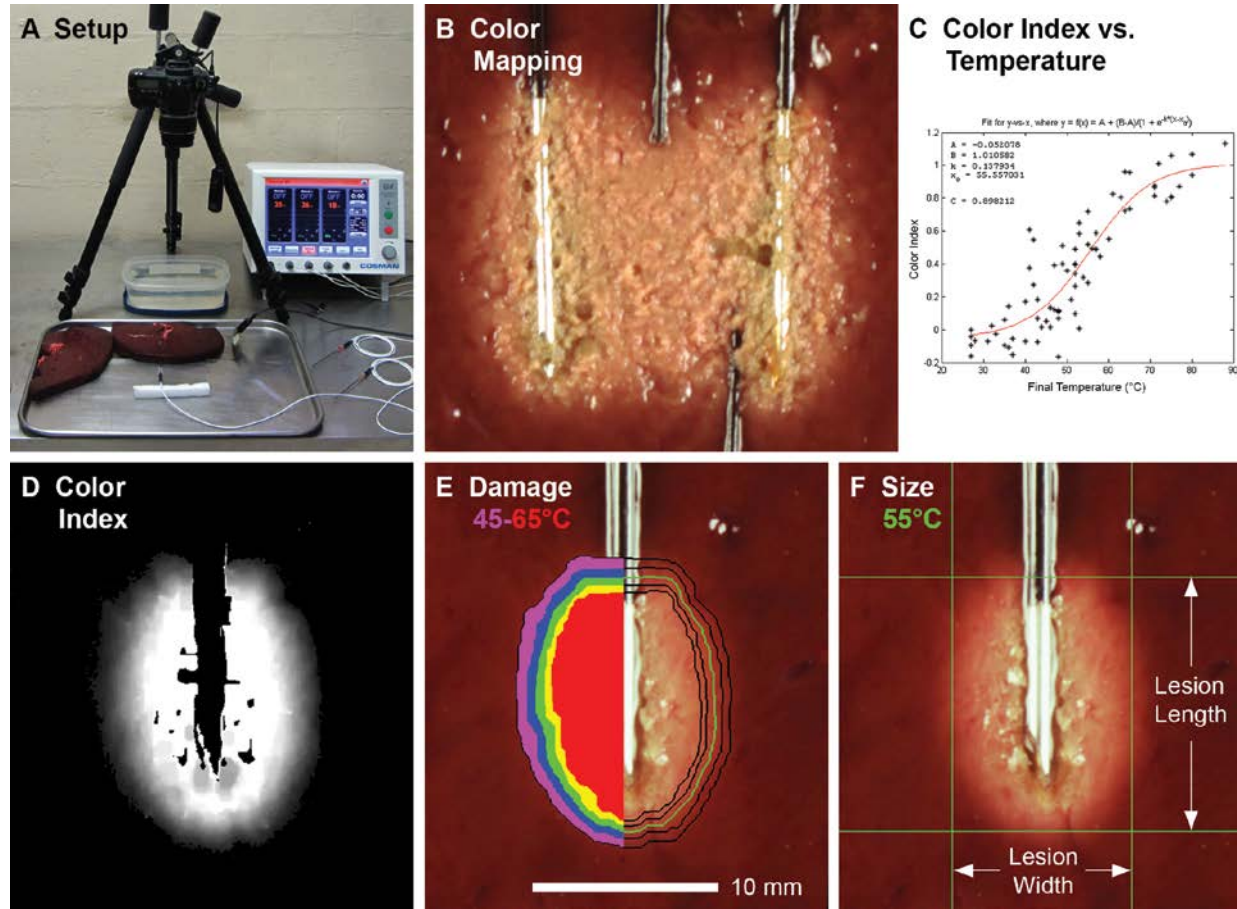


Figure 2 (A) Experimental setup for photographing RF lesions in ex vivo animal tissue. (B) Preliminary color/temperature mapping. Two temperature probes are shown within a 90°C/3 min bipolar lesion between 20 ga/15 mm tip cannulae spaced by 13–14 mm. (C) Color index demonstrates a logistic relationship to final temperature after 3 minutes heating. (D–F) Monopolar lesion size inference for an 18 ga/10 mm tip cannula at 90°C for 3 minutes. Thermal damage (E) is inferred from the color index image (D) by means of curve (C). Lesion length L and width W are determined at the 55°C damage level (F).

80°C (Figure 2C). A logistic curve fit to these data estimates a functional relationship $p = f(T)$ between tissue color index p and the thermal damage due to heating up to temperature T over 3 minutes.

Over 400 lesions are generated using a variety of electrode and generator configurations, and each is photographed for automated size measurement. Photographic scale is established by selection of points separated by 20 mm on the pictured ruler. The image is resampled to 20 pixels per millimeter and automatically rotated using cannula orientation inferred by peak detection in a Hough transform of the image [27,28]. The color index of the central-lesion cluster is adjusted using the known set temperature T_{set} , and thermal damage $T = f^{-1}(pf(T_{set}))$ is inferred for each pixel. The image is thresholded at the $T = 55^\circ\text{C}$ damage level. Fine imaging noise is reduced using a binary opening operation with a disc structuring

element of radius 7 pixels, and the largest connected component is identified as the heat lesion (Figure 2E). Monopolar lesion width W and length L are measured as the largest distance between lesion pixels in the vertical and horizontal image directions (Figures 1A and 3F). For bipolar lesions, midline width W , length L , and depth D are measured in addition to the maximal extent in the length L_{max} and depth D_{max} directions (Figure 1B). Lesion volume V is estimated from cross-sectional images by numerical integration, including the de minimus probe volume (e.g., $\approx 0.02 \text{ cm}^3$ for a 16 ga/10 mm cannula). Monopolar volume is computed by summing circular slices of varying width along the lesion length $V = \int \pi W^2 dL/4$. Bipolar volume is computed by summing elliptical slices of varying depth and length along the lesion width $V = \int \pi DL dW/4$.

Standard, sharp, bevel-tipped RF cannulae (Cosman CC10XY and RFK-C10XYS, 10 cm shaft, X mm tip length,



Figure 3 From top to bottom: a curved, sharp, bevel-tip RF cannula with stylet in place (20 ga/10 mm active tip, 10 cm shaft); a straight, sharp, bevel-tip RF cannula with stylet in place (20 ga/10 mm active tip, 10 cm shaft); an RF thermocouple electrode (10 cm nitinol shaft); the electrode positioned within the straight cannula's inner lumen; a trocar-tip "Ray" RRE electrode.

Y ga diameter, 18° bevel) and nitinol TC electrodes (Cosman TCN-10) are used to generate both monopolar and parallel-tip bipolar lesions (Figures 1 and 3). A unitized TC electrode/cannula with a sharp bevel tip and integral injection port is used for all 23 ga lesions (Cosman CU-10X23, 10 cm shaft, X mm tip length). The trocar-tipped "Ray" electrode (Cosman RRE, 16 ga/6 mm tip) is used to generate monopolar lesions. For these cases, the generator raises the tip temperature to within 5°C of the set temperature in about 10–15 seconds. Monopolar cooled RF lesions are generated with an 18 ga/4 mm tip internally cooled electrode (SInergy SIP-17-150-4, Baylis Medical Company, Inc., Montreal, QC, Canada) and its fully insulated 17 ga introducer (Baylis SII-17-150) using recommended settings [29–31]. In a pre-treatment cooling step, the Baylis RF generator (PMG-115-TD version 2.2A) and pump (TDA-PPU-1) circulate room-temperature fluid through the electrode for 45 seconds. After this, RF is applied for 2.5 minutes during which the tip temperature increases to 60°C with a linear ramp rate of 80°C/min. Pretreatment cooling is 5 seconds for subsequent lesions.

Sampling of electrode and generator configurations is organized into the following groups, centering on "common cannulae" with tip sizes 23 ga/5 mm, 22 ga/5 mm, 20 ga/10 mm, 18 ga/10 mm, 16 ga/10 mm (tip diameter/length), and generator settings 80°C/2 min (time/temperature), which appear in several groups:

- Tip size effects: Combinations of cannula tip diameters (23, 22, 20, 18, 16 ga) and lengths (5, 6, 10, 15 mm), and the RRE electrode (16 ga/6 mm tip trocar), at 80°C for 2 minutes.
- Temperature effects: Common cannulae at 60, 70, 80, 90°C for 2 minutes.
- Time effects: Common cannulae at 80°C for 1, 1.5, 2, 3, 5, 10 minutes.

- Combined effects: 16 ga/6 mm, 18 ga/10 mm, 16 ga/10 mm cannulae at 80–90°C for 2–3 minutes.
- Cooled RF: 18 ga/4 mm tip ramped to 60°C at 80°C/min over 2.5 minutes, plus 45 seconds pretreatment cooling [29–31].
- Bipolar RF: 20 ga/10 mm, 18 ga/10 mm, 16 ga/10 mm cannulae with 10–15 mm parallel tip spacing at 80–90°C for 2.5–3 minutes.

Five lesions are generated for each configuration in each group, and the dimensions of each lesion are measured by the automated system. Lesion size for each configuration is reported by averaging the measured dimensions of all samples of that configuration.

Results

Linear regression of monopolar lesion width W (mm) and length L (mm) measurements with respect to cannula tip diameter d (mm), tip length l (mm), set temperature T (°C), and set time t (minutes) produces the following models within the parameter ranges studied:

$$W = 4.02d + 0.09l + 0.14T + 0.35t - 10.44$$

$$L = 2.46d + 0.92l + 0.09T + 0.22t - 7.38$$

The correlation coefficients R^2 between model and data are 0.92 and 0.97, and the standard errors are 0.65 mm and 0.59 mm, respectively. Analysis of variance indicates high statistical significance for the overall models and for each regression coefficient individually (P values < 0.001). Model fit can be improved by adding regressors that account for size saturation as temperature and time increase.

Figure 4 plots the average and standard deviation of heat lesion width and length for each monopolar RF configuration generated using standard cannulae and TC electrodes, as well as the RRE electrode. Figure 5 shows these trends using photographs of representative lesions. Figure 5G shows examples of similar trends in bipolar heat lesions. Figure 6 shows large RF lesions produced by standard cannulae in monopolar and bipolar configurations and by the monopolar cooled RF configuration. Table 1 lists the standard deviation about the average dimensions of large lesions presented in Figures 4–6. Across all the configurations, the average configuration-specific standard deviation for lesion width is 0.41 mm (min 0.19 mm, max 0.75 mm), and for lesion length was 0.46 mm (min 0.14, max 0.95).

Tip Size Effects

For a sharp-tip cannula energized in a monopolar configuration, average lesion length is 0–5.8 mm longer than the tip length, the lower value corresponding to 60°C/2 min configurations and the upper value corresponding to 16 ga/10 mm/80°C/10 min (Figure 4 right). The briefer and more practical configuration 16 ga/6 mm/85°C/3 min

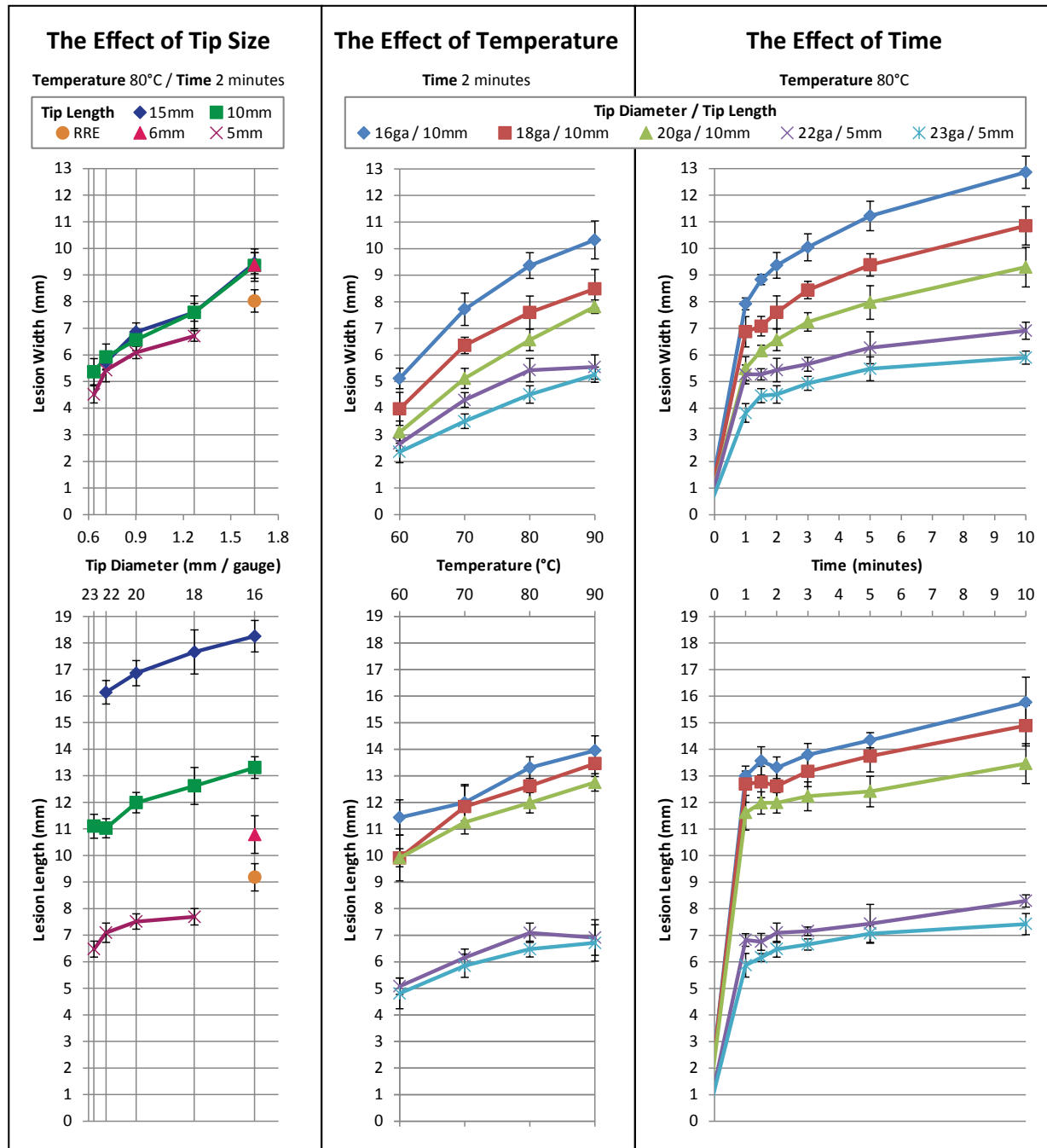
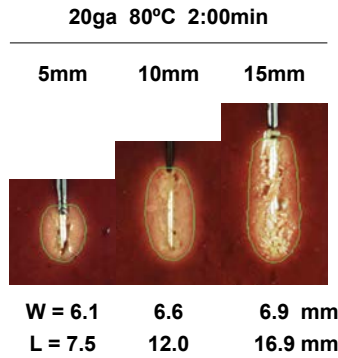
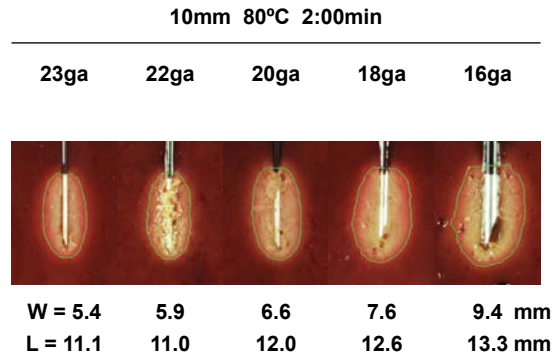


Figure 4 Average monopolar RF heat lesion width W (top) and length L (bottom) plotted as a function of tip diameter/gauge, tip length, set temperature, and set time for sharp RF cannulae/electrodes and the RRE “Ray” electrode. Error bars plot the standard deviation about the average dimension.

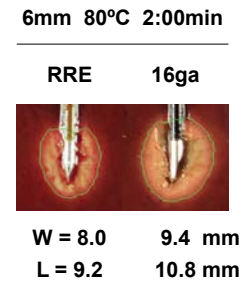
A Tip Length



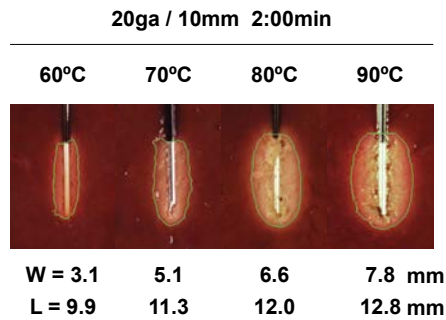
B Diameter / Gauge



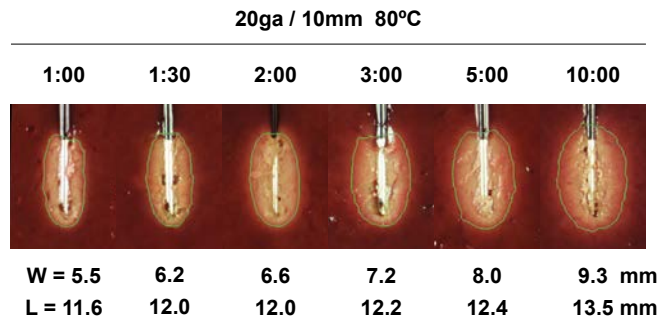
C Construction



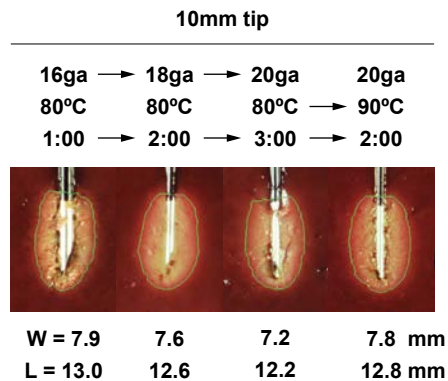
D Temperature



E Time



F Similar Lesions



G Bipolar RF (W x L)

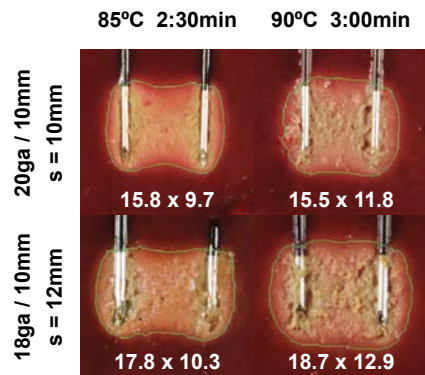
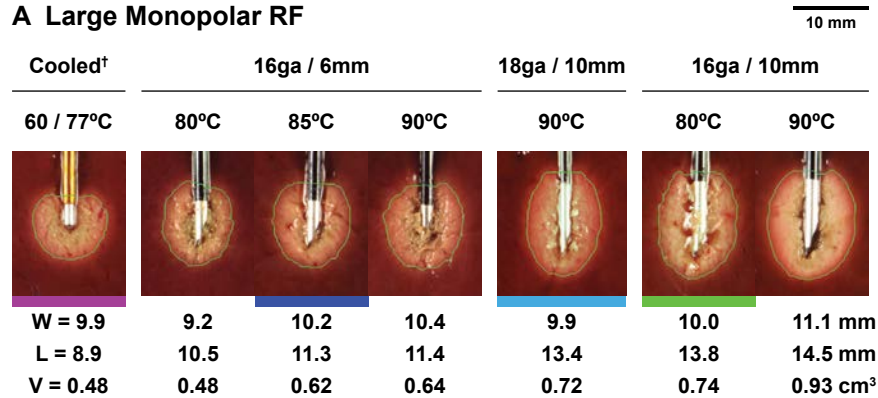
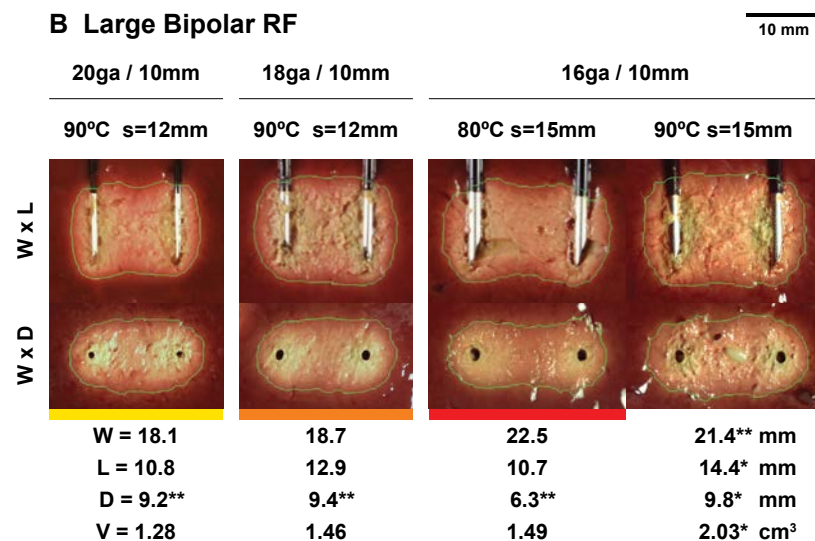


Figure 5 Average midline width W and length L of RF heat lesions created by sharp-tip RF cannula/electrodes. (A,B,D,E) Trends due to cannula tip length, diameter/gauge, temperature, and time, as plotted in Figure 4. (C) Comparison with RRE solid trocar electrode. (F) Higher temperature and/or longer lesion time can compensate for smaller cannula diameter in some cases. From left to right, the average lesion effective radii [21] are 3.1, 3.2, 3.2, and 3.5 mm. (G) Bipolar RF heat lesion size depends on tip spacing s in addition to tip length, diameter, temperature, and time. [25]. For each case shown, the maximum bipolar lesion length exceeds the midline length. From left to right, top to bottom, the average maximum lesion lengths are 11.8, 12.5, 11.9, and 13.8 mm.

A Large Monopolar RF**B Large Bipolar RF****C Monopolar vs. Bipolar RF**

- Bipolar 16ga/10mm 80°C
- Bipolar 18ga/10mm 90°C
- Bipolar 20ga/10mm 90°C
- Monopolar 16ga/10mm 80°C
- Monopolar 18ga/10mm 90°C
- Monopolar 16ga/6mm 85°C
- Cooled 18ga/4mm 60/77°C[†]

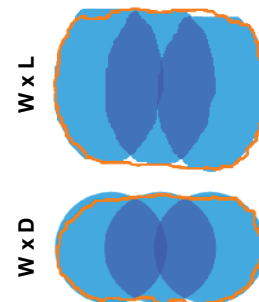
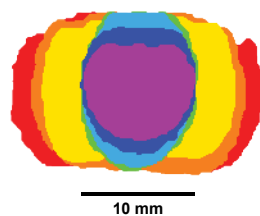


Figure 6 Average midline width W , length L , depth D , and volume V of large RF heat lesions for 3:15 minutes total time. This comprises a 15-second ramp plus 3 minutes at the set temperature for conventional lesions, or 45 seconds of pre-treatment cooling plus 2.5 minutes of RF heating for the cooled RF lesions. (A) Monopolar heat lesions. (B) Bipolar heat lesions with tip spacing s , shown in two cross sections. From left to right, the average maximal bipolar lesion lengths/depths are 12.6/9.6**, 13.8/9.7**, 13.5/9.4**, and 15.0*/11.0* mm. (C) Bipolar lesions compared with monopolar lesions at the minimal temperature achieving 10 mm average width. A sequence of three monopolar lesions approximate the shape of one bipolar lesion generated using the same cannulae, time, and temperature. *Value from one sample. **Value from two samples. [†]Tissue reaches 77°C when the 18 ga/4 mm cooled electrode measures 60°C.

Table 1 The average and standard deviation dimensions of large lesions presented in Figures 4–6

Modality	Tip diameter (ga)	Tip length (mm)	Temp (°C)	Time (minute)	Lesion width <i>W</i> (mm)	Lesion length (mm)		Lesion depth (mm)		Volume <i>V</i> (cm ³)
						Midline <i>L</i>	Maximal <i>L</i> _{max}	Midline <i>D</i>	Maximal <i>D</i> _{max}	
Cooled	18	4	60	2.5	9.9 ± 0.7	8.9 ± 0.5		N/A		0.48 ± 0.09
Monopolar	16	6	80	2	9.4 ± 0.6	10.8 ± 0.7		N/A		0.50 ± 0.08
Monopolar	16	6	80	3	9.2 ± 0.3	10.5 ± 0.5		N/A		0.48 ± 0.04
Monopolar	16	6	85	3	10.2 ± 0.2	11.3 ± 0.3		N/A		0.62 ± 0.04
Monopolar	16	6	90	3	10.4 ± 0.6	11.4 ± 0.4		N/A		0.64 ± 0.10
Monopolar	18	10	90	3	9.9 ± 0.4	13.4 ± 0.3		N/A		0.72 ± 0.07
Monopolar	16	10	80	2	9.4 ± 0.5	13.3 ± 0.4		N/A		0.62 ± 0.08
Monopolar	16	10	80	3	10.0 ± 0.5	13.8 ± 0.4		N/A		0.74 ± 0.11
Monopolar	16	10	90	2	10.3 ± 0.7	14.0 ± 0.6		N/A		0.81 ± 0.14
Monopolar	16	10	90	3	11.1 ± 0.6	14.5 ± 0.2		N/A		0.93 ± 0.10
Bipolar <i>s</i> = 10 mm	20	10	85	2.5	15.8 ± 0.2	9.7 ± 0.5	11.8 ± 0.2	†		
Bipolar <i>s</i> = 10 mm	20	10	90	3	15.5 ± 0.2	11.8 ± 0.7	12.5 ± 0.5	†		
Bipolar <i>s</i> = 12 mm	20	10	90	3	18.1 ± 0.7	10.8 ± 0.3	12.6 ± 0.3		9.2†	1.28 ± 0.04
Bipolar <i>s</i> = 12 mm	18	10	85	2.5	17.8 ± 0.5	10.3 ± 0.4	11.9 ± 0.1	†		
Bipolar <i>s</i> = 12 mm	18	10	90	3	18.7 ± 0.3	12.9 ± 0.6	13.8 ± 0.3		9.4†	1.46 ± 0.08
Bipolar <i>s</i> = 15 mm	16	10	80	3	22.5 ± 0.3	10.7 ± 0.6	13.5 ± 0.2		6.3†	1.49 ± 0.10
Bipolar <i>s</i> = 15 mm	16	10	90	3	21.4†	14.4*	15.0*		9.8*	2.03*

* Value from one sample.

† Value from two samples.

‡ No data.

Bipolar tip spacing is denoted *s*.

Table 2 Average and standard deviation lesion dimensions as a joint function of temperature and time

18 ga/10 mm			16 ga/10 mm		
Lesion width W (mm)		2 minutes	3 minutes		
	80°C	7.6 ± 0.6	8.4 ± 0.3	80°C	9.4 ± 0.5
	90°C	8.5 ± 0.7	9.9 ± 0.4	90°C	10.3 ± 0.7
Lesion length L (mm)		2 minutes	3 minutes		
	80°C	12.6 ± 0.7	13.2 ± 0.6	80°C	13.3 ± 0.4
	90°C	13.5 ± 0.5	13.4 ± 0.3	90°C	14.0 ± 0.6

Data for two cannula tip sizes shown in Figures 4 and 6A

produces an average lesion length 5.3 mm longer than the tip exposure (Figure 6A). A heat lesion extends proximal and distal to the active tip in roughly equal proportion. Lesion width is somewhat enlarged by increasing tip length from 5 mm to 15 mm (Figures 4 left, 5A, and 6A).

Increasing cannula diameter increases lesion length and width (Figures 4 left and 5B). Because the increase in lesion width is greater than the increase in tip diameter, there is also an increase in the radial extent of lesioned tissue, termed the effective radius [21]. For example, increasing cannula diameter from 23 ga to 16 ga increases average lesion width by 4.0 mm (74%) from 5.4 mm to 9.4 mm, and lesion length by 2.2 mm from 11.1 mm to 13.3 mm, for a 10 mm tip at 80°C and 2 minutes (Figures 4 left and 5B). This corresponds to an increase in the maximum effective lesion radius $(W-d)/2$ of 1.5 mm (63%) from 2.4 mm to 3.9 mm. Diameter d depends on gauge as follows: 16 ga = 1.65 mm, 17 ga = 1.47 mm, 18 ga = 1.27 mm, 19 ga = 1.07 mm, 20 ga = 0.91 mm, 22 ga = 0.71 mm, 23 ga = 0.64 mm.

The 16 ga/6 mm trocar-tipped RRE electrode produces smaller average lesion size $W \times L$ (8.0 mm \times 9.2 mm) than a standard bevel-tipped cannula/electrode of equivalent dimension (9.4 mm \times 10.8 mm) for the same generator settings 80°C/2 min (Figures 4 left and 5C).

Temperature Effects

For the monopolar RF cannulae studied, increasing set temperature from 60°C to 90°C increases average lesion width by 2.9–5.2 mm (108–152%), and average lesion length by 1.8–2.8 mm at 2 minutes, excluding the apparently anomalous value for the 18 ga/10 mm tip cannula at 60°C (Figures 4 center and 5D). For example, width increases from 5.1 mm to 10.3 mm, and length from 11.4 mm to 14.0 mm, for the average 16 ga/10 mm tip cannula.

Time Effects

Across studied cannulae at 80°C, although monopolar lesions grow most rapidly over the first minute, average lesion width is 0.7–1.4 mm (11–20%) larger at 2 minutes, and 1.1–2.1 mm (23–32%) larger at 3 minutes, as com-

pared with 1 minute (Figures 4 right and 5E). Average lesion length is 0.1–0.5 mm larger at 2 minutes, and 0.3–0.8 mm larger at 3 minutes, compared with 1 minute, as assessed by quadratic fit to configuration-specific averages. Lesion width and length continue to increase throughout the observation time of 10 minutes.

Combined Effects

For the monopolar RF cannulae configurations investigated, tip length, tip diameter, temperature, and time each independently increases lesion size. For example, in Figure 4 (left), increasing tip length in the range 5–15 mm, or tip diameter in the range 23–16 ga, increases lesion size even if the other is already increased. In Figure 4 (center and right), lesion dimensions enlarged by increasing tip size are further enlarged by increasing either temperature or lesion time. Figures 4 and 6A show several cases in which average lesion dimensions increase with temperature and time in the ranges 80–90°C and 2–3 minutes, even if the other factor is already increased. Two of these cases are summarized in Table 2, wherein the effect is more pronounced for width than for length. Figure 6A, Tables 1 and 2 show the effect of increasing all factors simultaneously: average lesion width approaches or exceeds 10 mm for some configurations of 16 ga/6 mm, 18 ga/10 mm, and 16 ga/10 mm cannula in the ranges 80–90°C and 2–3 minutes.

Cooled RF

Figure 6A (left) shows a lesion produced by the cooled RF configuration wherein the 18 ga/4 mm tip is heated to 60°C over 2.5 minutes following 45 seconds of pre-treatment cooling, as recommended [29–31]. This configuration produces a slightly oblate ellipsoidal lesion with average width 9.9 mm and average length 8.9 mm. Consistent with published in vivo measurement [13], direct temperature probing around the active tip indicates 77°C maximum tissue temperature when the internally cooled electrode measures 60°C.

Bipolar RF

For the parallel bipolar configurations studied, average lesion width exceeds the tip spacing by 5.5–7.5 mm and

is about twice that of a monopolar lesion produced using the same generator settings and cannula size (Figure 6C right). Using bipolar generator settings 85°C/2.5 min, 20 ga/10 mm cannulae spaced by 10 mm produce a single, rounded, brick-shaped lesion with average width 15.8 mm (Figure 5G left). With the same settings, 18 ga/10 mm cannulae spaced by 12 mm produce an analogous lesion shape with average width 17.8 mm (Figure 5G left). With similar generator settings 80°C/3 minutes, 16 ga/10 mm cannulae spaced by 15 mm produce a similar lesion shape with average width 22.5 mm (Figure 6B). Increasing temperature and time to 90°C/3 min for each of these configurations enhances midline lesion length and depth, producing more convex lesions (Figures 5G right and 6B). Bipolar generator settings 90°C/3 min produce average midline lesion depths of 9.2–9.8 mm, and average maximum lesion depths of 9.6–11.0 mm, for studied configurations (Figure 6B).

Discussion

Tip Size, Temperature, and Time Effects

The results of this study show that monopolar RF lesion width and length vary considerably over the range of cannula tip sizes and generator settings currently available for interventional pain management. Lesion length increases in proportion to cannula tip length in the range 5–15 mm. Heating lateral, distal, and proximal to the active tip is enhanced by use of larger diameter, higher temperature, and longer lesion time. Lesions generated by thin (23, 22 ga) and thick (18, 16 ga) cannula differ sizably in all dimensions (e.g., Figure 5B). The same is true of lesions generated at low (60–70°C) and high (80–90°C) temperatures (e.g., Figure 5D). Although the predominance of lesion growth occurs within the first minute of monopolar RF heating, growth continues over the second and third minutes of heating as well, particularly for larger cannula. This suggests that lesion times of 2–3 minutes are practical means of lesion size enlargement for standard monopolar RF, just as they are for cooled RF and bipolar RF [25,29,30].

Large monopolar RF lesions can be generated using conventional cannulae by maximizing all factors within practical limits: 16 ga/6 mm, 18 ga/10 mm, or 16 ga/10 mm tip size; 80–90°C set temperature; and 2–3 minutes lesion time (Figures 4 and 6A, and Tables 1 and 2). Lesion size may be further enhanced by pre-lesion injection of saline or lidocaine through the cannula, as suggested by D. A. Provenzano et al. [32]. Although not fully quantified in the present study due to limited post-lesion tip visibility, conventional monopolar RF lesions can have considerable extension both distal and lateral to the cannula's distal point (Figures 6A and 7). This observation does not revise the fundamental conclusion by N. Bogduk et al. that a monopolar heat lesion produced by an elongated active tip generally has a greater lateral than distal extent [21]. However, it does suggest that increasing tip diameter, tip length, temperature, and/or time can reduce technical failures due to directional and/or translational misalign-

ment between a cannula and nerve. Furthermore, larger conventional monopolar lesions may be useful for neurotomies of the T5–T8 medial branch nerves, which float in inter-transverse spaces with poor reference to bony landmarks [33], or for point-on approaches where the nerve and cannula can be directly visualized with ultrasound guidance.

The data indicate some cases in which thinner cannula can produce lesions of equivalent dimension to those produced by thicker cannula, by means of increasing lesion temperature and/or time. Similarly, there are cases where intervention time can be reduced by means of higher temperature and/or larger tip diameter. For example, Figure 5F shows cases in which 20 ga, 18 ga, and 16 ga cannula produce similar lesion sizes, including similar effective radii, for different temperature and time settings. The data and trends plotted in Figure 4 provide a basis for identification of such equivalences, which can be verified through clinical study.

Lesions produced by the solid 16 ga/6 mm trocar-tipped RRE electrode appear to be somewhat smaller than those produced by a standard bevel-tipped cannula/electrode of the same dimension (Figure 5C). Standard 16 ga/6 mm or 18 ga/10 mm sharp-tip cannulae may be considered as an alternative to the RRE electrode for cervical medical branch neurotomy procedures using the posterior approach [34,35].

Cooled RF

Previous publications on sacroiliac joint (SIJ) denervation using cooled RF report 8–10 mm as the range of lesion widths produced by a 18 ga/4 mm/60°C/2.5 min cooled RF configuration and in ex vivo chicken muscle [29], and clinically near the bony surface of the human sacrum [13]. The present study is limited to this one cooled RF configuration as a point of comparison with other RF configurations. The average lesion width 9.9 mm found in the present study is at the upper end of the previously reported range. The tissue temperature 77°C measured around the cooled active tip in the present study is similar to the reported maximum in vivo tissue temperature 75°C measured around the cooled active tip near the human sacrum clinically [13].

Internal cooling of an RF electrode substantially increases heat lesion size. This is well known and strongly evidenced by cooled RF electrodes used for tumor ablation, which produce lesions of 20–50 mm width, much larger than is achievable with conventional RF [10–12]. However, the present study underscores the fact that some conventional RF lesions are larger than some cooled RF lesions. Just as a conventional lesion generated by a 22 ga/5 mm tip cannula at 70°C for 1 minute has very different dimensions from those generated by a 16 ga/10 mm tip cannula at 90°C for 3 minutes, the relative sizes of conventional and cooled RF lesions depend on the parameters of each configuration.

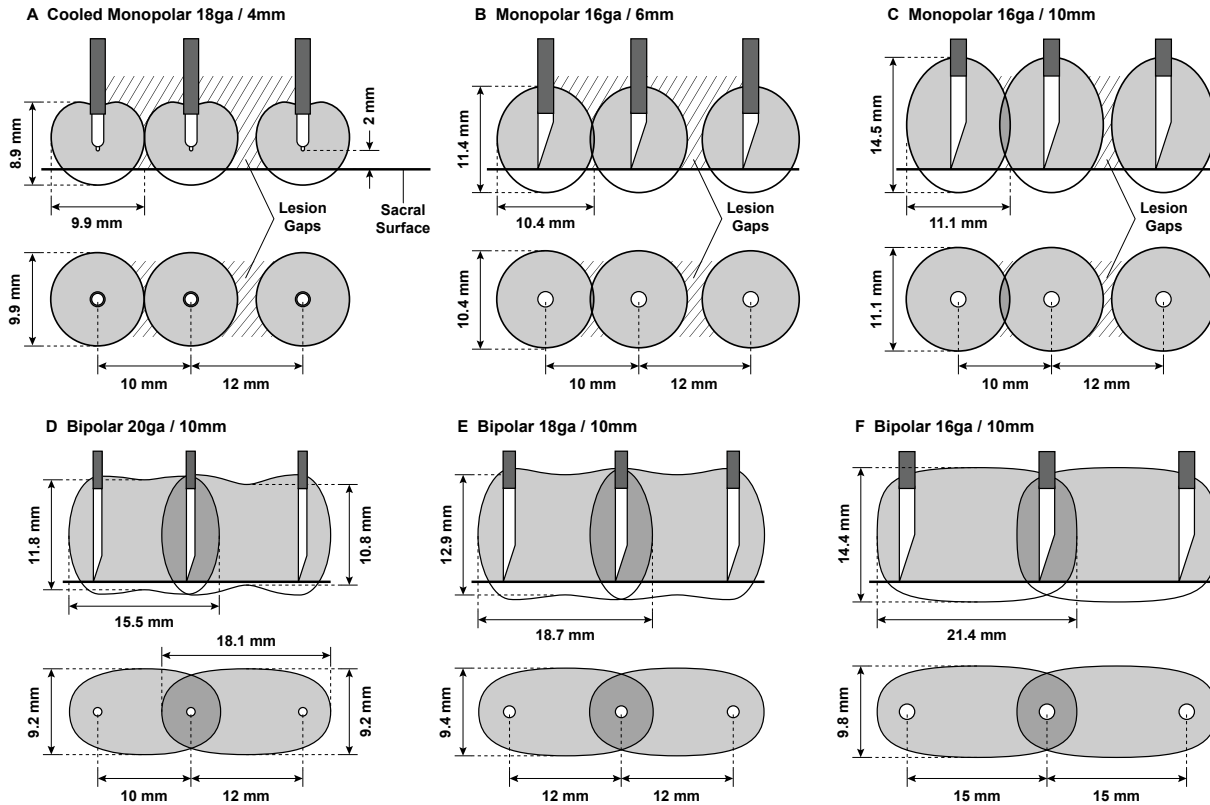


Figure 7 Comparison of sequential monopolar and bipolar heat lesioning with tips perpendicular to the idealized surface of a vertebral bone, such as the dorsal sacrum. (A–C) The thickness of the aggregate lesion produced by sequential monopolar lesions can vary substantially if inter-tip spacing exceeds the lesion width. (D–F) With proper selection of generator settings and tip size, sequential bipolar lesions that share a common electrode position produce aggregate lesions of consistent height and width without gaps over a range of spacings. Lesion sizes are derived from data in Figures 5 and 6, using settings 90°C/3 min for all conventional configurations (B–F). The cooled RF introducer stylet is 2 mm longer than the electrode, so the electrode is suspended 2 mm from the surface [30].

Figure 6A, Tables 1 and 2 present examples of conventional monopolar RF configurations that produce similar or larger average lesion sizes than the studied monopolar cooled RF configuration. These conventional and cooled setups resemble each other in aspects that are clinically relevant: the diameter of the insertion cannula (17 ga for the cooled RF, 18–16 ga for conventional), the total time involved in lesion generation including all ramp and pre-treatment cooling times (3:15 seconds for both cooled and conventional RF), the lesion time itself (2:30 minutes for cooled RF, 2–3 minutes for conventional), and the maximum tissue temperature (approximately 77°C for cooled RF, 80–90°C conventional). However, the presented examples do not strictly control for these parameters. In some cases, the differences reflect fundamental trade-offs that will not be resolved by a lesion-size study, but only by consideration of procedural objectives, clinical outcomes, and complications.

The range of cooled RF probes and generator settings in clinical pain management publications is limited at present. However, a variety of cooled RF configurations are possible. Increasing tip length, tip diameter, lesion time and control temperature, injecting saline and lidocaine, and using bipolar RF are each expected to increase the size of cooled RF heat lesions, as they do for conventional RF heat lesions.

Bipolar RF

In a previous study, E. R. Cosman Jr. and C. D. Gonzalez demonstrate the dependency of bipolar lesion geometry over a range of tip diameters (22, 20, 18 ga), tip lengths (5, 10, 15 mm), set temperatures (60, 70, 80, 90°C), set times (0.5–10 minutes), and tip spacings (2–20 mm), and they characterize the robustness of inter-lesion heating to various departures from ideal parallel tip alignment [25].

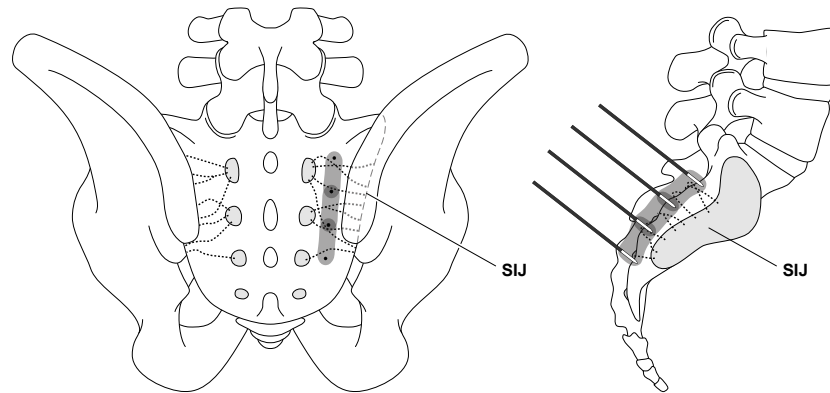


Figure 8 Palisade bipolar heat lesioning of the sacral lateral branch nerves for treatment of sacroiliac joint (SIJ) pain. Four 16 ga/10 mm tip cannula, spaced by approximately 15 mm, are lowered to the dorsal sacral surface along a line between the lateral aspect of the sacral foramina and the ipsilateral SIJ. A series of three bipolar lesions at 90°C/3 min are generated between each pair of adjacent cannulae to lesion the space through which the sacral lateral branch nerves travel at irregular locations [36]. This is a theoretical modification of a method used clinically in which a greater number of thinner cannula span the same anatomical region with closer spacing, namely five or six 20 ga/10 mm or 18 ga/10 mm cannula spaced by 10–12 mm [25].

The present study is limited to small number of bipolar configurations as points of comparison with other RF configurations. There is close agreement between the ex vivo lesion shapes and dimensions produced by configurations included in both the present and previous study, though the present study shows somewhat larger lesion depths *D* due to an improved measurement method. The present ex vivo study shows lesion formation at the inter-tip location corresponding to previous in vivo temperature measurements of 53–64°C between two bipolar 20 ga/10 mm cannulae spaced by 10–12 mm and heated at 90°C for 3 minutes near the human sacrum [25].

With proper selection of cannula size and generator settings, bipolar RF produces rounded brick-shaped heat lesions that surround substantially parallel cannulae spaced up to 10–15 mm or more. This bipolar lesion shape is similar to that of a closely-spaced sequence of three monopolar lesions produced using the same generator settings and cannula size (Figure 6C right). Estimated bipolar lesion volume is similar to that of two of the monopolar lesions (Table 1). Even for relatively thin cannulae, bipolar lesions can be considerably larger than the largest lesions produced by conventional and cooled monopolar RF (Figures 5G and 6, Table 1). However, bipolar RF requires at least two cannula placements for each lesion, and the relative sizes of particular monopolar and bipolar lesions depend on the particular parameters of each configuration.

Bipolar RF's asymmetric lesion shape and robustness to variations in tip spacing may offer advantages over monopolar RF's axially symmetric lesion shape for the creation of elongated heat lesions of consistent height and

thickness (Figure 7). These advantages may come without substantial drawbacks when bipolar RF replaces monopolar RF in a method that already involves the generation of two or more lesions. For example, a clinical report of the multi-bipolar Palisade method for posterior SIJ denervation uses five or six 20 ga/10 mm or 18 ga/10 mm cannula positions, and four or five inter-cannula bipolar lesions, to span the region through which sacral lateral branch nerves reside with irregular number and variable positions relative to bony landmarks [25,36]. This reduces both the number of lesions and the cannula diameter relative to the reported monopolar cooled RF approach, in which eight lesions are generated using a 17 ga cannula and 18 ga/4 mm active tip [29–31]. Results from the present study suggest that use of larger 16 ga/10 mm cannula could reduce the number of cannula positions to four, and the number of inter-cannula bipolar lesions to three (Figure 8), but this has not been evaluated clinically.

Previous ex vivo and in vivo investigations show a wider variety of bipolar configurations than the present study and include setups that produce smaller bipolar lesions that may be more appropriate in some applications [25]. Increasing tip length, tip diameter, lesion time and set temperature, and injecting saline and lidocaine [37] are each expected to increase the size of bipolar RF heat lesions, as they do for monopolar RF heat lesions.

Large Lesions

Increasing heat lesion size has well-known theoretical advantages and disadvantages, whether conventional, cooled, or bipolar RF is used. Larger lesions can reduce

the likelihood of missing a target nerve [2,23,35] and increase the number and extent of target nerves captured by each lesion. This may help to avoid incomplete neurolysis, to improve the degree and duration of pain relief, and to reduce procedure time, x-ray exposure, and the number of required lesions. However, larger lesions may also increase the likelihood and severity of damage to nontarget nerves, skin burns in thin patients, and postprocedural paresthesia [35,38]. Some of these side effects may be related to the volume of affected tissue, which varies considerably across the lesions generated in the present study. For example, the estimated volumes of the large lesions listed in Table 1 are 4–20 times greater than that generated by the classic SMK configuration 22 ga/5 mm/80°C/1.5 min ($0.10 \pm 0.01 \text{ cm}^3$). Even within Table 1, the largest monopolar lesion is 90% larger than the cooled RF lesion, and the bipolar lesions are 2.5–4 times larger than the cooled RF lesion, on average. The volume of affected tissue is also a function of the number of lesions needed to reliably interrupt a target nerve (which fortuitously tends to decrease as individual lesion volume increases) and the degree of lesion overlap. Though serious complications are rare, they should be considered when lesion size or number is increased in order to improve outcomes, as should other means for avoiding treatment failure such as improved targetry, patient selection, and diagnosis [38–41]. The results of the present study provides guidance about how lesions size and shape can be adjusted to investigate these trade-offs clinically.

Comparison with Other Ex Vivo Lesion Size Studies

Many prior studies use homogeneous ex vivo animal tissue to assess RF lesion size. Adult bovine liver [25,42], bovine muscle [21,23,25], porcine muscle [25,43], chicken muscle [25,29,32,37], and chicken egg white [20–22,25,44,45] are common ex vivo models. In previous studies, lesion size is measured manually using apparent tissue color change. The variety of tissue types and measurement methods used in prior studies confounds comparison of different configurations across studies. The present study is unique in that color change is empirically correlated to thermal damage, and lesion size is measured using an automated system to reduce human measurement bias and to assess a wide variety of configurations in single tissue model.

Among the solid animal tissues bovine liver, bovine muscle, porcine muscle, and chicken muscle, it appears that the choice of tissue type does not largely affect trends in the size of temperature-controlled RF heat lesions. Nor would this be expected given their analogous electrical and thermal properties [44]. Though the absolute lesion sizes measured in this and other bovine liver studies [25,42] are generally larger than those measured in some animal muscle studies [21,23,29,32,37], the trends are similar in both cases. Although this offset in apparent lesion size may reflect actual differences in the tissue temperature pattern, it may also be linked to differences in the way tissue color indicates thermal exposure and dif-

ferences in the way investigators define the lesion boundary relative to color. Direct tissue temperature measurement for equivalent RF lesioning configurations suggests that temperature-controlled RF heating patterns are similar for solid tissue types but that bovine liver produces more pronounced color change in response to lower temperatures (45–50°C) than do animal muscles [25,43]. As such, bovine liver can discriminate temperatures over the full range thought to be neurolytic clinically and can image aspects of a thermal exposure pattern that may be invisible or faint in some other tissue types. In the present study, this property of bovine liver is measured empirically and used to automatically determine lesion boundaries based on the relationship between tissue color and thermal exposure (Figure 2B and C).

Lesion sizes reported in the present study, and in other studies using solid animal tissue, are generally larger than those reported in studies that use chicken egg white [20–22,25,44,45]. Egg white is a convenient tool for real-time visualization of heat lesions and can be used to demonstrate some heat lesion properties, including fine high-temperature details [44]. However, egg white exhibits pronounced fluid convection dynamics that are absent in solid tissue targets clinically and ex vivo [25]. Egg white also changes color only at high temperatures (62–65°C [46]), obscuring lower temperatures linked to clinical neurolysis. These properties may explain smaller lesion sizes in egg white, by the reasoning that convection in egg white carries more weakly heated fluid up and away from a growing lesion before it can be further heated and change color [25]. They may also explain other unusual characteristics of egg white lesions that are neither predicted by theoretical lesion models [44], nor exhibited in solid animal tissue ex vivo: egg white lesions tend not to extend distal to cannula tips that are pointed downward even though temperatures are highest there [44]; egg white lesions do not grow appreciably after 60–90 seconds in standard monopolar setups [20,22]; and bipolar egg white lesions do not form a single connected volume between 22 ga/5 mm tip cannulae spaced by more than about 6 mm and heated to 90°C for 3 minutes [25,45]. Given these discrepancies and physical considerations, solid animal tissue is expected to be a more clinically applicable ex vivo model for lesion size assessment than egg white.

Comparison with In Vivo Lesion Size Studies

A review of prior investigations of RF lesion size in vivo [4,13,17–20,25] provides some evidence that ex vivo lesions in the present study are predictive of those generated in actual interventional pain management procedures. In vivo temperature measurements around an 18 ga/4 mm tip cooled RF electrode near the human sacrum suggest an 8–10 mm lesion width and a maximum tissue temperature of 75°C when the tip measures 60°C after 2.5 minutes of RF application [13]. The present study finds the same configuration produces a 9.9 mm average lesion width and a maximum tissue temperature of 77°C. In vivo

temperature measurements are reported in the range 53–64°C at the dorsal surface of the human sacrum, midway between bipolar 20 ga/10 mm tip cannula lowered point-on to that surface, spaced by 10–12 mm, and heated to 90°C for 3 minutes [25]. The present study shows lesion formation at the corresponding location for the same configurations *ex vivo*. Monopolar lesions in the living human brain generated using 16 ga/10 mm blunt-tip electrodes at 80–90°C for 1 minute are reported to be 10 mm wide and 10–12 mm long when assessed 6 months postmortem [18,19]. In the present study, 16 ga/10 mm sharp-tip cannulae/electrodes generate lesions 7.9-mm wide by 13.0-mm long at 80°C/1 min and exceed 10 mm width between 80 and 90°C at 2 minutes. Monopolar lesion width produced by 19 ga/5 mm round-tip electrodes in the living monkey brain is reported to increase by 4.5 mm (87%) from 5.2 mm to 9.7 mm as tip temperature is varied from 60 to 90°C for 2 minute lesion time, when assessed 0–14 weeks postmortem [17]. In the present study, lesion width produced by monopolar 18 ga/10 mm cannulae/electrodes increases by 4.5 mm (113%) from 4.0 mm to 8.5 mm over the same range.

Limitations

The size of lesions generated in *ex vivo* and cadaveric models may differ from those generated in clinical practice due to differing electrothermal properties, blood flow, tissue hydration, tissue homogeneity, initial temperature, injected fluids, and the imprecise relation between clinical neurolysis and experimental indicators of lesioned tissue (e.g., color, temperature, and time). For example, higher initial tissue temperature (e.g., 37°C vs 24°C) is expected to increase clinical lesion size. Active blood flow is expected to limit lesion size, particularly at longer lesion times when weaker heating in the peripheral lesion cannot coagulate capillaries [44]. Lesion shape may be affected clinically by variations in tissue properties around target nerves in the spine, which can include thin cortical bone, trabecular bone with red marrow, muscle, fascia, ligament, tendon, fat, various intravertebral tissue types, blood vessels, cerebrospinal fluid, other nerves, injected fluids, spinal hardware, and other heat lesions. The present study does not model or quantify the net impact of these discrepancies from clinical practice. No one homogeneous medium may be most representative. Though it would be useful to study the effect of spinal tissue inhomogeneity, anatomical variations, and variations in electrode position in a cadaveric, animal, or clinical spinal model, the present study is limited to a homogeneous *ex vivo* model to avoid obscuring the effects of studied factors. Given the unknown clinical applicability of any *ex vivo* model, this and other *ex vivo* RF lesion studies are best understood in terms of relative trends, rather than absolute dimensions.

Sources of error in the present study may include variation in tissue and photographic characteristics, displacement of temperature probe location, misalignment between active tip and photographed cross section, spatial variation in thermal damage, variation in baseline tissue tem-

perature, image processing error, small sample size for configuration-specific averages, and indirect measurement of lesion volume.

Conclusions

In the present study, automated photographic analysis is used to compare monopolar RF heat lesion size across cannula diameters, active tip lengths, set temperatures, and set times available for interventional pain management. All four factors are found to significantly affect heat lesion size. Heating both lateral and distal to the active tip is enhanced by means of larger cannula diameter, higher tip temperature, and/or longer duration RF application. Lesion size continues to increase even after 60–90 seconds of sustained heating, often used clinically. In some cases, increasing temperature and/or time enables a thinner cannula to generate lesion dimensions similar to those produced by a thicker cannula at lower temperature or shorter time. Comparison with the solid RRE “Ray” electrode suggests standard cannula sizes that could be used in the method of cervical medial branch neurotomy introduced by S. M. Lord and collaborators for the treatment of chronic cervical zygapophysial joint pain [23,34,35,47]. With proper selection of generator settings, monopolar RF using a standard 18 ga or 16 ga cannulae produces heat lesions of average widths comparable with those of the cooled RF heat lesions proposed for treatment of SIJ pain [29,30]. Comparison with parallel-tip bipolar RF (Figure 1B) confirms that bipolar lesion sizes can be much larger than those of monopolar RF, as suggested in previous *ex vivo* and clinical study in the context of SIJ pain treatment [25].

References

- 1 Cosman ER Sr, Cosman ER Jr. Radiofrequency lesions. In: Lozano AM, Gildenberg PL, Tasker RR, eds. *Textbook of Stereotactic and Functional Neurosurgery*, 2nd edition. Berlin/Heidelberg: Springer-Verlag; 2009:1359–82.
- 2 Bogduk N, ed. *Practice Guidelines for Spinal Diagnostic and Treatment Procedures*. San Francisco, CA: International Spine Intervention Society; 2004.
- 3 Brodkey JS, Miyazaki Y, Ervin FR, Mark VH. Reversible heat lesions with radiofrequency current: A method of stereotactic localization. *J Neurosurg* 1964;21:49–53.
- 4 Dieckmann G, Gabriel E, Hassler R. Size, form, and structural peculiarities of experimental brain lesions obtained by thermocontrolled radiofrequency. *Confin Neurol* 1965;26:134–42.
- 5 Smith HP, McWhorter JM, Challa VR. Radiofrequency neurolysis in a clinical model. *Neuropathological correlation*. *J Neurosurg* 1981;55:246–53.
- 6 Hamann W, Hall S. Acute effect and recovery of primary afferent nerve fibres after graded RF-lesion

- in anaesthetized rats. *Br J Anaesth* 1992;68: 443P.
- 7 Frohling MA, Schlote W, Wolburg-Buchholz K. Non-selective nerve fibre damage in peripheral nerves after experimental thermocoagulation. *Acta Neurochir (Wien)* 1998;140:1297–302.
- 8 Podhajsky RJ, Sekiguchi Y, Kikuchi S, Myers RR. The histologic effects of pulsed and continuous radiofrequency lesions at 42 degrees C to rat dorsal root ganglion and sciatic nerve. *Spine (Phila Pa 1976)* 2005;30:1008–13.
- 9 Dreyfuss P, Halbrook B, Pauza K, et al. Efficacy and validity of radiofrequency neurotomy for chronic lumbar zygapophysial joint pain. *Spine* 2000;25: 1270–7.
- 10 Goldberg SN, Gazelle GS, Solbiati L, Rittman WJ, Mueller PR. Radio-frequency tissue ablation: Increased lesion diameter with a perfusion electrode. *Acad Radiol* 1996;3:636–44.
- 11 Solbiati L, Goldberg SN, Ierace T, et al. Hepatic metastases: Percutaneous radio-frequency ablation with cooled-tip electrodes. *Radiology* 1997;205:367–73.
- 12 Goldberg SN, Solbiati L, Hahn PF, et al. Large volume tissue ablation with radio frequency by using a clustered, internally cooled electrode technique: Laboratory and clinical experience in liver metastases. *Radiology* 1998;209:371–9.
- 13 Wright RF, Wolfson LF, DiMuro JM, Peragine JM, Bainbridge SA. In vivo temperature measurement during neurotomy for SIJ pain using the Baylis SInergy probe. *International Spine Intervention Society 15th Annual Scientific Meeting*: 82–84; 2007.
- 14 Sweet WH, Mark VH. Unipolar anodal electrolyte lesions in the brain of man and cat: Report of five human cases with electrically produced bulbar or mesencephalic tractotomies. *AMA Arch Neurol Psychiatry* 1953;70:224–34.
- 15 Hunsperger RW, Wyss OAM. Qualitative Ausschaltung von Nervengewebe durch Hochfrequenzkoagulation. *Helv Physiol Pharmacol Acta* 1953;11:283–304.
- 16 Von Bonin G, Alberts WW, Wright EW Jr, Feinstein B. Radiofrequency brain lesion size as a function of physical parameters. *Arch Neurol (Chicago)* 1965;12:25–9.
- 17 Alberts WW, Wright EW Jr, Feinstein B, Von Bonin G. Experimental radiofrequency brain lesion size as function of physical parameters. *J Neurosurg* 1966;25(4): 421–3.
- 18 Cosman ER, Nashold BS, Bedenbaugh P. Stereotaxic radio frequency lesion making. *Appl Neurophysiol* 1983;46(1):160–6.
- 19 Cosman ER, Nashold BS, Ovelman-Levitt J. Theoretical aspects of radiofrequency lesions in the dorsal root entry zone. *Neurosurgery* 1984;15:945–50.
- 20 Vinas FC, Zamorano L, Dujovny M, et al. In vivo and in vitro study of the lesions produced with a computerized radiofrequency system. *Stereotact Funct Neurosurg* 1992;58:121–33.
- 21 Bogduk N, Macintosh J, Marsland A. A technical limitation to efficacy of radiofrequency neurotomy for spinal pain. *Neurosurgery* 1987;20:529–35.
- 22 Moringlane JR, Koch R, Schäfer H, Ostertag ChB. Experimental radiofrequency (RF) coagulation with computer-based on line monitoring of temperature and power. *Acta Neurochir (Wien)* 1989;98(3–4):126–31.
- 23 Lord SM, McDonald GJ, Bogduk N. Review article: Percutaneous radiofrequency neurotomy of the cervical medial branches—A validated treatment for cervical zygapophysial joint pain. *Neurosurg Q* 1998;8:288–308.
- 24 Cosman ER. Thermocouple Radio Frequency Lesion Electrode. U.S. Patent 4,411,266. Filed Sep 24, 1980. Issued Oct 25, 1983.
- 25 Cosman ER Jr, Gonzalez CD. Bipolar radiofrequency lesion geometry: Implications for palisade treatment of sacroiliac joint pain. *Pain Pract* 2011;11:3–22.
- 26 Chang I, Nguyen U. Thermal modeling of lesion growth with radiofrequency ablation devices. *Biomed Eng Online* 2004;3:27.
- 27 Hough PVC. Machine Analysis of Bubble Chamber Pictures. *Proc Int Conf High Energy Accelerators and Instrumentation*; 1959.
- 28 Duda RO, Hart PE. Use of the hough transform to detect lines and curves in pictures. *Commun ACM* 1972;15:11–5.
- 29 Cohen SP, Hurley RW, Buckenmaier CC III, et al. Randomized placebo-controlled study evaluating lateral branch radiofrequency denervation for sacroiliac joint pain. *Anesthesiology* 2008;109:279–88.
- 30 Kapural L, Nageeb F, Kapural M, et al. Cooled radiofrequency system for the treatment of chronic pain from sacroiliitis: The first case-series. *Pain Pract* 2008;8:348–54.
- 31 SInergy System User Guide PM1013 rev 09/08. Montreal, Canada: Baylis Medical Company, Inc.; 2008.

- 32 Provenzano DA, Lassila HC, Somers DL. The effect of fluid injection on lesion size during radiofrequency treatment. *Reg Anesth Pain Med* 2010;35:338–42.
- 33 Chua WH, Bogduk N. The surgical anatomy of thoracic facet denervation. *Acta Neurochir (Wien)* 1995;136:140–4.
- 34 MacVicar J, Borowczyk JM, MacVicar AM, Loughnan BM, Bogduk N. Cervical medial branch radiofrequency neurotomy in New Zealand. *Pain Med* 2012;13:647–54.
- 35 Govind J, King W, Bailey B, Bogduk N. Radiofrequency neurotomy for the treatment of third occipital headache. *J Neurol Neurosurg Psychiatry* 2003;74(1):88–93.
- 36 Yin W, Willard F, Carreiro J, Dreyfuss P. Sensory stimulation-guided sacroiliac joint radiofrequency neurotomy: Technique based on neuroanatomy of the dorsal sacral plexus. *Spine* 2003;28:2419–25.
- 37 Provenzano DA, Lutton EM, Somers DL. The effects of fluid injection on lesion size during bipolar radiofrequency treatment. *Reg Anesth Pain Med* 2012;37:267–76.
- 38 Cohen SP, Chen Y, Neufeld NJ. Sacroiliac joint pain: A comprehensive review of epidemiology, diagnosis and treatment. *Expert Rev Neurother* 2013;13(1):99–116.
- 39 Cohen SP, Bajwa ZH, Kraemer JJ, et al. Factors predicting success and failure for cervical facet radiofrequency denervation: A multi-center analysis. *Reg Anesth Pain Med* 2007;32(6):495–503.
- 40 Cohen SP, Hurley RW, Christo PJ, et al. Clinical predictors of success and failure for lumbar facet radiofrequency denervation. *Clin J Pain* 2007; 23(1):45–52.
- 41 Cohen SP, Strassels SA, Kurihara C, et al. Outcome predictors for sacroiliac joint (lateral branch) radiofrequency denervation. *Reg Anesth Pain Med* 2009;34(3):206–14.
- 42 Goldberg SN, Gazelle GS, Dawson SL, et al. Tissue ablation with radiofrequency: Effect of probe size, gauge, duration, and temperature on lesion volume. *Acad Radiol* 1995;2:399–404.
- 43 Derby R, Lee CH. The efficacy of a two needle electrode technique in percutaneous radiofrequency rhizotomy: An investigational laboratory study in an animal model. *Pain Physician* 2006;9:207–14.
- 44 Cosman ER Jr, Cosman ER Sr. Electric and thermal field effects in tissue around radiofrequency electrodes. *Pain Med* 2005;6(6):405–24.
- 45 Pino CA, Hoefft MA, Hofsess C, Rathmell JP. Morphologic analysis of bipolar radiofrequency lesions: Implications for treatment of the sacroiliac joint. *Reg Anesth Pain Med* 2005;30:335–8.
- 46 Yang S-C, Baldwin RE. Functional properties of eggs in foods. In: Stadelman WJ, Cotterill OJ, eds. *Egg Science and Technology*. Binghamton, NY: Haworth Press; 1995:405–64.
- 47 Lord SM, Barnsley L, Wallis BJ, McDonald GJ, Bogduk N. Percutaneous radio-frequency neurotomy for chronic cervical zygapophyseal-joint pain. *N Engl J Med* 1996;335:1721–6.